Research Article

DOI: 10.1002/jst.84

Mechanics of flight in ski jumping: aerodynamic stability in pitch

Pascual Marqués-Bruna[1,*] *and Paul Grimshaw*[2]

[1] *Faculty of Arts and Sciences, Edge Hill University, Ormskirk, UK*
[2] *School of Mechanical Engineering, University of Adelaide, Australia*

This study examines aerodynamic stability in pitch in ski jumping. Static stability implies automatic return to trimmed flight after a sudden disturbance and dynamic stability involves gradual damping of oscillatory motion. Both have implications for flight control and safety. A 3-D inertia model of a ski jumper and the Planica K185 jumping hill profile were constructed using computer-aided design. Inertia, jump performance, and aerodynamic efficiency and stability parameters were computed for variations in V-style posture using mathematical modeling. Pitching moment at a 0° angle of attack was positive, and the condition $dM/d\alpha < 0$ *at equilibrium was satisfied, indicating that the athlete is inherently stable. Enhanced flight posture consists of a ski-opening angle of 30° and a forward-leaning angle of 10°. This is a high-lift configuration with a large static margin that triggers a steep* $dM/d\alpha$ *slope and high oscillatory frequency upon deviations from trimmed attitude. Mechanisms of stability in pitch are proposed, founded upon theoretical aerodynamics.* © *2009 John Wiley and Sons Asia Pte Ltd*

Keywords:
- aerodynamics
- computer-aided design
- modeling
- ski jumping
- stability

1. INTRODUCTION

The ability to maintain a stable attitude is essential to flight. Static stability implies capability to automatically return to trimmed flight after a sudden disturbance [1,2]. Thus, if the angle of attack (α) is temporarily increased, aerodynamic forces produce a nose down pitching moment (M). A system that is aerodynamically unstable tends to diverge, and neutral stability implies no response to the new flight attitude [3,4]. Balance implies the ability to reach equilibrium (zero net M) at a trim angle of attack (α_0) (Figure 1; based on Nelson [3]). The principle for static pitch stability is that $dM/d\alpha < 0$ at equilibrium (negative curve slope) [5]. However, the angle between the ski jumper's zero-lift line and the oncoming flow (α_w) must be positive at equilibrium in order to produce useful lift. Static stability refers only to the direction of the system's initial response to a disturbance, while dynamic stability involves gradual damping of a disturbance over time [3,6].

Stability in pitch is known as longitudinal stability about the lateral (y) axis (Figure 2), stability in roll is termed lateral stability about the longitudinal (x) axis, and stability in yaw is called directional stability about the normal (z) axis [2]. Lateral motion depends on cross-coupling of roll and yaw [7]; however, longitudinal stability can be assessed independently. We might expect to find different postural configurations of the ski jumper that vary in terms of aerodynamic efficiency [8,9] and longitudinal stability [10].

Airfoil theory and principles of aircraft stability [e.g. 1,4,6,7] may be used to examine stability mechanisms in ski jumping. An orthodox positively-cambered airfoil produces an aerodynamic nose down moment, and is therefore unstable. In contrast, a reflexed cambered airfoil produces a positive moment. Thus, a tailless aircraft design needs a reflexed airfoil shape with the centre of gravity (CG) ahead of the aerodynamic centre (AC) so that a nose-up disturbance produces an increase in lift behind the CG and restores trimmed attitude. Moving the CG forward lengthens the static margin

*Faculty of Arts and Sciences, Edge Hill University, St Helen's Road, Ormskirk, Lancashire, L39 4QP, United Kingdom.
E-mail: Marquesp@edgehill.ac.uk

© 2009 John Wiley and Sons Asia Pte Ltd

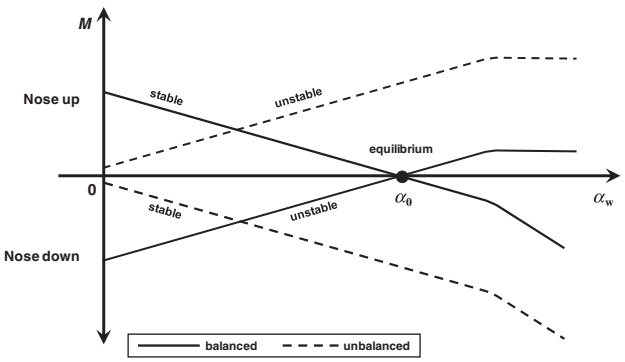

Figure 1. Four possible profiles of M as a function of α_w.

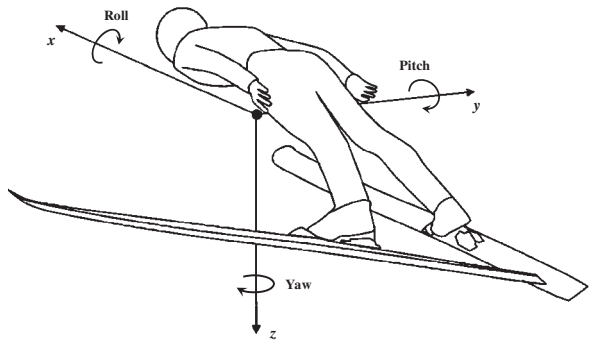

Figure 2. Six degrees of freedom along and about the three orthogonal principal axes of the ski jumper with origin at the *CG* (positive senses are in the directions shown).

(*SM*; distance between the *CG* and the *AC*) and increases static stability. According to Katz [11], the *AC* for a thin arc-shaped, negatively-cambered airfoil at $\alpha = 0^\circ$ is near quarter chord, whereas the centre of pressure (*CP*) is aft of the *AC*, at half chord. Thus, in a condition of zero net lift, positive lift due to incidence (F_{Linc}; acting at the *AC*) forms a positive aerodynamic couple with the negative lift due to camber (F_{Lcam}; acting at the *CP*). The efficiency and stability of airfoils and wings is dictated ultimately by flow regime, critical Reynolds number (Re_{crit}), and downwash, wake, and vortex configuration [1,4,12,13]. The ski jumper–skis system is comprised of lifting surfaces, whereby such principles of aeronautics may apply.

Past research in ski jumping has focused on flight posture and lift mechanisms [9,13], and recommendations for ski length and jumping hill design for improved safety [e.g. 8,14–16]. Very few studies [e.g. 10,13] have examined oscillatory pitching motion. Uppermost, the mechanisms of static stability in pitch in ski jumping have not been explicated. Theoretical approximations of inertial properties of the ski jumper and aerodynamic behavior may be obtained using computer-aided design (CAD) and mathematical modeling. Thus, the aims of this study are to: (i) model aerodynamic efficiency and aerodynamic stability according to flight posture; and (ii) identify the mechanisms of stability in pitch in ski jumping. This notional knowledge will contribute to safety in the sport.

2. METHOD

2.1 Hypothetical Ski Jumper and Competition Conditions

The virtual ski jumper had a mass, including equipment, of 70 kg and a height of 1.76 m [10], and used commercially available skis of 2.57 m length (146% of athlete's height), 11.5 cm width, and ski bindings (boot tip to ski tip distance of 57% of ski length). The equipment complied with Fédération Internationale de Ski [17] specifications. The following angles determine the posture of the ski jumper (based upon Meile *et al.* [8], Schwameder [9], and Müller *et al.* [14,15]). The ski opening angle (λ) (Figure 3) was set at 20°, 25° and 30°. The forward leaning angle (θ) was sampled from 0 to 40° at 10° intervals. Hip angle (β) was held at 0° (based on the wind tunnel database of Seo *et al.* [10]), and the arm abduction angle was constant at 10° (arms held to the sides of the body). Simulation of competition levels incorporated freestream air velocities (V_a) of 20 m/s (typical at takeoff in medium jumping hills), 25 m/s (large hills) and 30 m/s (ski flying hills) [15–17]. Air density (ρ) was assumed to be 1.18 kg/m^3 [10], and air temperature (T) 0°C.

2.2 CAD Model, Inertia Parameters, and Jumping Hill Profile

A 14-segment 3-D isometry solid model of the ski jumper [18,19] was designed using Delcam PowerSHAPE-e 8080 CAD software, anthropometric data adjusted for 3-D modeling [20] and postural ski-jumping flight data [e.g. 8,9,14,21]. Coordinates for segmental landmarks were obtained to the nearest millimeter. The position of the *CG* and the principal moment of inertia (I_y; parallel axes theorem; Equation 1 in Appendix 1) were computed for each flight posture [18,22]. Inertial properties of the helmet, boots, and skis (five additional segments) were included using equations for symmetric objects of uniform composition (Equations 2 and 3 [19]). The ski tips were assumed to bend upward during flight [10] creating negatively cambered profiles. The coordinates for the Planica K185 jumping hill [17] were plotted using CAD for the computation of flight trajectory, flight time (t_f) and jump length (ℓ_j).

2.3 Definitions of Aerodynamic Variables

The direction of flight path (φ) is expressed by the projectile velocity (V) vector (Figure 3). V_a is opposite in direction to V. α is the angle between the skis and V_a [15]. α_0 represents equilibrium for longitudinal oscillatory motion [10], and the stall angle (α_{ST}) is the angle beyond which lift declines (based on Kermode [1] and Bertin [12]). M is the net rotational effect of aerodynamic forces around the y axis [7]. Nose-up M is defined as positive [2]. Angular acceleration ($\ddot{\alpha}$) around α_0 is induced by aerodynamic moments during out-of-trim flight [3]. The *CP* is an abstract theoretical concept that signifies the nomadic point of application of resultant aerodynamic pressure forces [4]. In trimmed flight, the *CP* was assumed collinear

 © 2009 John Wiley and Sons Asia Pte Ltd

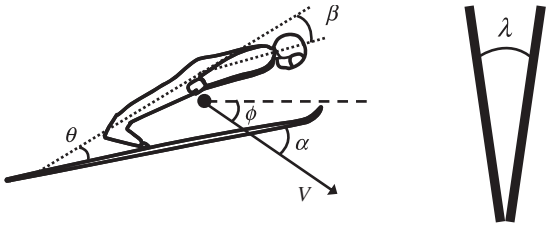

Figure 3. Configuration of the ski jumper and λ in flight.

to the *CG*. The centre-of-pressure shift (ΔCP) represents the translation of the *CP* along the pseudo chord as α varies (adapted from Anderson [2]). The pseudo chord epitomizes the amalgamation of the chords of individual lifting surfaces (e.g. body, skis); based on Carpenter [5]. The *AC* is the point along the chord at which pitching moment is constant regardless of α [12], and applies to individual lifting surfaces (e.g. one ski only). The neutral point (*NP*) has the same mechanical meaning as the *AC*; however, it applies when two or more lifting surfaces are considered simultaneously [5]. *SM* is the distance from the *NP* to the *CG* [6]. For the theoretical analysis, lift force was divided into two parallel components. F_{Lcam} was considered to act at the *CG*, and F_{Linc} was set to act at the *NP* (founded on Simons [4] and Thomas & Taylor [7]). Two dynamic stability parameters were obtained. The period of the short-period mode (T_{sp}) is the time for one complete cycle of oscillatory motion around α_0, and frequency (f) represents the reciprocal of T_{sp} [3,5].

2.4 Calculation of Aerodynamic Parameters, Flight Trajectory, and Jump Performance

Aerodynamic parameters for systematic variations in ski jumping posture were computed for $\alpha = 0°$–$50°$ at $0.5°$ intervals. Drag force (F_D), lift force (F_L), lift-drag ratio (F_L/F_D) and M were calculated, for which drag area (C_DA) lift area (C_LA) and moment volume (Q_M) were estimated using polynomial equations from Seo *et al.* [10] based on wind tunnel data (Equations 4–6). The estimation error when using such equations has been reported as being within $\pm 4\%$ for C_DA and C_LA, and $\pm 9\%$ for Q_M (Seo *et al.* [10]). Reynolds number (*Re*) was approximated using Equation 7 [12,23]. Flight trajectory was computed using equations of motion for the ski jumper (Equations 8 and 9 [14–16]), and a fourth-order Runge–Kutta iterative method at 0.001-s intervals [24,25]. It was assumed that the athlete maintained aerodynamic posture from 0.6 s after takeoff to just before landing [8] and sustained trimmed flight for each posture (see Table 1). t_f and ℓ_j were established using the intersection of the flight path and the hill profile as the landing point. ΔCP was computed using Equation 10 (adapted from Anderson [2]). The $dM/d\alpha$ slope (from α_0 to $\alpha_0+0.5°$) was computed and displayed graphically. $\ddot{\alpha}$, *SM*, T_{sp} and f were computed using Equations 11–14 (based on Nelson [3], Carpenter [5] and Seo *et al.* [10]).

Table 1. α_0 and theoretical t_f and ℓ_j according to athlete's posture and V_a.

			$V_a = 20$ m/s		$V_a = 25$ m/s		$V_a = 30$ m/s	
λ (°)	θ (°)	α_0 (°)	t_f (s)	ℓ_j (m)	t_f (s)	ℓ_j (m)	t_f (s)	ℓ_j (m)
20	0	20	4.02	96.2	6.95	211.2	8.54	295.5
	10	26	3.98	94.0	6.74	197.0	8.51	279.7
	20	28	3.83	89.6	5.95	167.5	7.91	250.2
	30	28	3.76	87.3	5.10	140.0	6.94	221.8
	40	28	3.47	80.7	4.33	117.8	5.81	181.0
25	0	19	4.15	99.8	7.79	234.1	9.03	315.1
	10	23	4.16	99.0	7.27	216.8	8.89	296.4
	20	25	3.91	91.8	6.19	176.5	8.17	262.0
	30	27	3.75	87.3	5.36	148.4	7.12	219.9
	40	30	3.31	77.1	4.16	112.8	5.43	168.9
30	0	18	4.48	107.8	8.57	262.8	9.84	348.8
	10	21	4.26	101.2	7.76	226.3	9.19	308.3
	20	23	4.11	96.8	6.58	190.4	8.42	271.9
	30	27	3.70	86.0	5.22	144.2	6.99	223.9
	40	34	3.28	76.3	3.81	103.4	4.98	153.9

2.5 Statistical and Theoretical Analyses

The relative contribution of postural and aerodynamic parameters λ, θ, α_0, F_L and F_D to variables ℓ_j and M was assessed using two stepwise multiple regression analyses $p < 0.05$ in SPSS [26]. An analysis of the mechanisms that determine stability in flight in ski jumping was carried out founded upon aerodynamics theory [3,5,6].

3. RESULTS

3.1 Inertia Parameters

The mean $\pm$ SD position of the *CG* for variations in flight posture was 54.9% $\pm$ 0.2% of the athlete's height and 1.8 $\pm$ 0.4 cm anterior to the trunk longitudinal axis. The mean $\pm$ SD I_y was 14.7 $\pm$ 0.3 kg m^2, where I_y increased with θ (thus, $I_y = 14.3$ kg m^2 for $\theta = 0°$, but $I_y = 15.1$–15.3 kg m^2 for $\theta = 40°$) and decreased slightly with λ (maximum difference between postures of 0.2 kg m^2).

3.2 Aerodynamic Forces, Reynolds Number, and Jump Performance

Figure 4 shows F_L, F_D and F_L/F_D for a selected V_a of 25 m/s. The position of α_0 and α_{ST} along the curves is shown. F_D increases monotonically from $\alpha \approx 10°$. F_L/F_D peaks at $\alpha = 2°$–$12°$, at which F_L is rather low. α_0, α_{ST} and F_L/F_D were independent of V_a; however, F_L and F_D increased exponentially with the square of V_a. Approximate *Re* was 1.73×10^5, 2.17×10^5 and 2.60×10^5 for $V_a = 20$, 25 and 30 m/s, respectively. The shortest theoretical t_f and ℓ_j were attained with posture $\lambda = 30°$ and $\theta = 40°$ and the longest with $\lambda = 30°$ and $\theta = 0°$ (Table 1).

© 2009 John Wiley and Sons Asia Pte Ltd

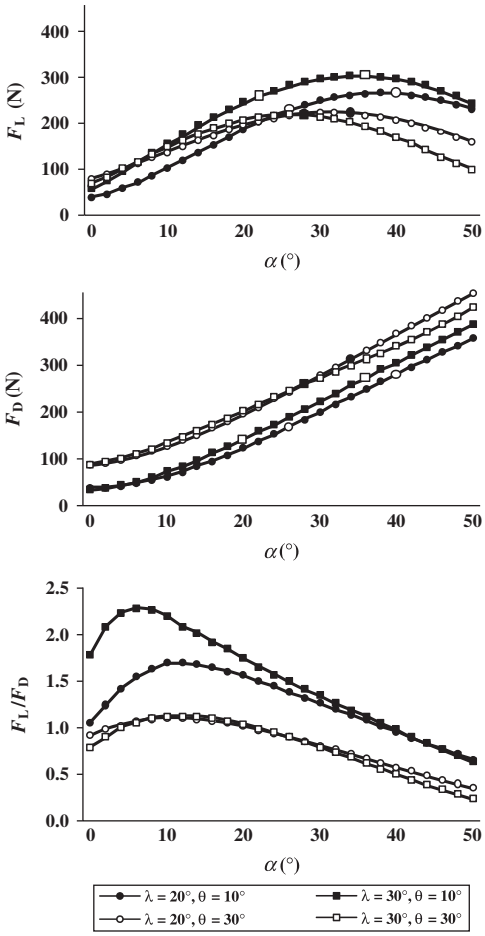

Figure 4. Aerodynamic forces and F_L/F_D as a function of athlete's posture and flight attitude.

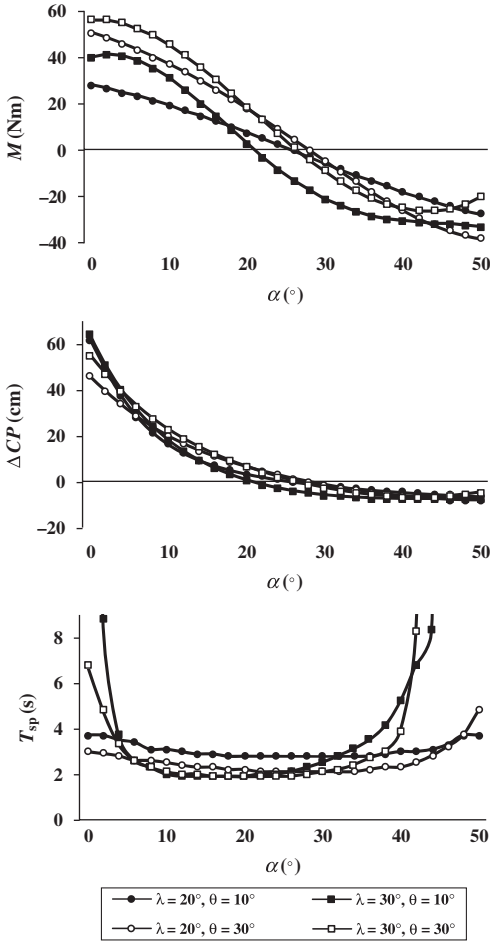

Figure 5. M, ΔCP and T_{sp} according to athlete's posture and flight attitude.

3.3 Aerodynamic Stability

Figure 5 displays M, ΔCP and T_{sp}. Equilibrium is attained at a positive α and the sign of the function $dM/d\alpha$ is negative. Balanced flight occurs within the range of $\alpha_0 = 18°$ (posture of $\lambda = 30°$ and $\theta = 0°$) and 34° ($\lambda = 30°$ and $\theta = 40°$; Table 1). The $dM/d\alpha$ slope becomes steeper as λ and θ increase, ranging from -0.82 Nm/° for $\lambda = 20°$ and $\theta = 0°$ to -2.67 Nm/° for $\lambda = 30°$ and $\theta = 40°$. ΔCP (forwards) is substantial at $\alpha < 10°$ and the CP remains within 10 cm aft of the CG at $\alpha > 25°$. Maximum nose-up $\ddot{\alpha}$ for out-of-trim flight ranged from 0.78 rad/s^2 (for $\lambda = 20°$ and $\theta = 0°$) to 4.39 rad/s^2 ($\lambda = 30°$ and $\theta = 40°$). M increased with the square of V_a and was thus influenced by hill size. In contrast, ΔCP was independent of V_a and was affected only by α. SM generally increased as a function of λ and θ, and was shortest for $\lambda = 20°$ and $\theta = 0°$ (2.3 cm) and longest for posture $\lambda = 30°$ and $\theta = 10°$ (7.2 cm); values were based on $V_a = 25$ m/s. $\lambda = 30°$ reduced T_{sp} for flight at $8° < \alpha < 26°$ (Figure 5). However, outside this range of α values the relatively flat $dM/d\alpha$ slopes for postures defined by $\lambda = 30°$ extend T_{sp} considerably. f increased as a function of λ and θ, and was lowest for $\lambda = 20°$ and $\theta = 0°$ (0.29 Hz) and highest for $\lambda = 20°$ and $\theta = 40°$ (0.53 Hz), showing approximately half a cycle per second (0.51 Hz) for $\lambda = 30°$ and $\theta = 10°$; values were based on $V_a = 25$ m/s. T_{sp} decreased, thus f increased non-linearly with V_a. Inertia and aerodynamic parameters for an enhanced posture of $\lambda = 30°$ and $\theta = 10°$ are shown in Table 2.

3.4 Statistical and Theoretical Analyses

In the first stepwise multiple regression test, F_L was entered first and explained 74% of the variance in ℓ_j ($F_{1,43} = 123.90$, $P = 0.001$, $\beta = 0.80$). θ had a negative correlation with ℓ_j ($\beta = -0.29$), was entered second and explained a further 8% ($F_{1,42} = 18.09$, $P = 0.001$). In the second test, F_D was entered first and explained 73% of the variance in M ($F_{1,43} = 115.74$, $P = 0.001$, $\beta = 0.75$). λ was entered second and explained a further 9% ($F_{1,42} = 21.63$, $P = 0.001$, $\beta = 0.29$), and F_L was entered third, which explained an additional 7% ($F_{1,41} = 26.92$, $P = 0.001$, $\beta = 0.29$). Figure 6 depicts the mechanisms of aerodynamic stability in pitch, where the dotted line represents the pseudo chord of the ski jumper–skis system.

 © 2009 John Wiley and Sons Asia Pte Ltd

4. DISCUSSION

4.1 CAD Model and Inertia Parameters

CAD is becoming an expedient tool in computational fluid dynamics (e.g. [8]). In our study, CAD permitted modeling variations in ski jumping posture. Incremented λ marginally shifted the *CG* forward along the x axis and concomitantly decreased I_y. In contrast, increased θ shifted the *CG* aft and prominently increased I_y. Moving the *CG* forward increases *SM* and overall static stability [6]. However, the *CG* position varied little with flight posture, indicating that *SM* depends primarily upon $dM/d\alpha$. The effects of inertial properties must be interpreted with caution. I_y may be regarded as a *damping derivative* and not an aerodynamic stabilizing factor, since I_y does not cause a return to α_0 but merely slows the departure from trimmed attitude [2,5]. However, once the disturbance has taken place, greater rotational inertia makes the system less responsive (less agile [5]). In this sense, greater I_y reduces f, which may be interpreted as lower static stability, but better damping of dynamic oscillations.

Table 2. Inertia and aerodynamic parameters for enhanced posture $\lambda = 30^\circ$ and $\theta = 10^\circ$.

	$V_a = 20$ m/s	$V_a = 25$ m/s	$V_a = 30$ m/s
I_y (kg m^2)	14.4	14.4	14.4
CG (% of height)	54.8	54.8	54.8
α_0 (°)	21	21	21
F_{Lcam} (N)	37	57	82
F_{Linc} (N)	124	194	279
F_L (N)	161	251	361
F_D (N)	95	148	213
F_L/F_D	1.7	1.7	1.7
$dM/d\alpha$ (Nm/°)	−1.70	−2.61	−3.83
SM (cm)	4.4	7.2	9.8
T_{sp} (s)	2.4	2.0	1.6
f (Hz)	0.42	0.51	0.63

4.2 Analysis of Flight Efficiency

Postures defined by $\lambda = 30^\circ$ and $\theta = 0^\circ$–10° are high-lift configurations (Figure 4) that result in the longest jumps (Table 1). In contrast, postures of $\lambda = 20^\circ$ and $\theta = 0^\circ$–10° produce only moderate lift and worsen F_L/F_D. Augmented lift with wide λ has been attributed to increased projected area under the ski jumper [13]; this effect is also enhanced by keeping the arms by the body (minimum arm abduction angle). The diminished lift for $\lambda = 20^\circ$ may be due to the blanketing of lifting surfaces (e.g. hands) immersed in the low-pressure wake of the skis [8]. Large λ generally augments drag; however, drag is predominantly a function of θ. Increased θ also brings α_0 closer to the stall. The first regression analysis confirms the importance of adopting high-lift postures [9], where it is essential to reduce θ for a long jump. Thus, $\lambda = 30^\circ$ and

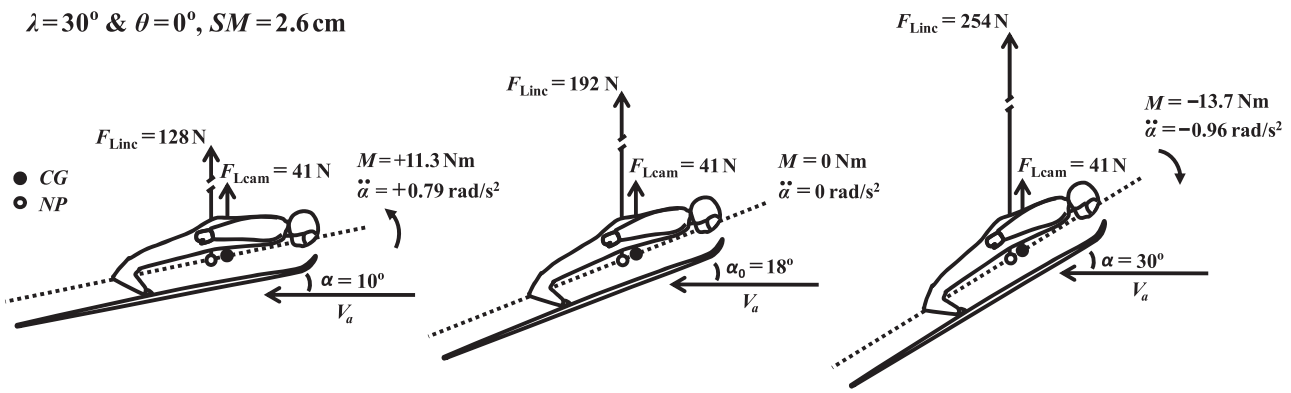

$\lambda = 20^\circ$ & $\theta = 0^\circ$, $SM = 2.3$ cm

$\alpha = 10^\circ$	$\alpha_0 = 20^\circ$	$\alpha = 30^\circ$
$F_L = 82$ N	$F_L = 155$ N	$F_L = 218$ N
$M = +7.8$ Nm	$M = 0$ Nm	$M = -7.7$ Nm
$\ddot{\alpha} = +0.55$ rad/s^2	$\ddot{\alpha} = 0$ rad/s^2	$\ddot{\alpha} = -0.54$ rad/s^2

$\lambda = 30^\circ$ & $\theta = 10^\circ$, $SM = 7.2$ cm

$\alpha = 10^\circ$	$\alpha_0 = 21^\circ$	$\alpha = 30^\circ$
$F_L = 154$ N	$F_L = 251$ N	$F_L = 296$ N
$M = +30.9$ Nm	$M = 0$ Nm	$M = -20.8$ Nm
$\ddot{\alpha} = +2.15$ rad/s^2	$\ddot{\alpha} = 0$ rad/s^2	$\ddot{\alpha} = -1.44$ rad/s^2

Figure 6. Theoretical analysis of balance and stability in ski jumping (based on $V_a = 25$ m/s).

© 2009 John Wiley and Sons Asia Pte Ltd

$\theta = 0°$–$10°$ yield better jump performance. β is a camber-changing device and theory advocates [3] that camber augmentation enhances the effective α, through chord line repositioning, and thus maximum lift coefficient. Ito *et al*. [13] have observed that the airfoil shape created by β decreases the area of flow separation and extends the glide. Thus, β should be adjusted according to V_a. Meile *et al*. [8] and Ito *et al*. [13] have found $\beta \approx 10$–$20°$ to be the most efficient. Ito *et al*. [13] and Reisenberger *et al*. [23] have observed that the flow around the back of the ski jumper is in the post-critical regime, typical of bluff bodies. It possesses therefore high momentum and results in late flow separation and reduced vortex shedding. The low Re_{crit} makes the torso of the athlete an efficient lifting surface, where the reduced vortex shedding may also help with stability. The flow field behind the skis has also been studied by Ito *et al*. [13]. Longitudinal tip vortices develop at the ski tips and circumvent from underneath, around the outside, and to the upside of the ski. The conical 3-D vortex flow from the right and left skis interact, and the flow produces downwash directly behind the ski jumper. In 3-D flow field, the low pressure tip vortices generate lift forces, like in a delta wing [11]. However, lift in ski jumping is essentially created by the downwash caused by 3-D tip vortex [13]. Thus, aerodynamic efficiency in ski jumping depends upon postural adjustment of λ and θ (as lift-generating factors), fine tuning of β (as a camber-changing device), and also on the nature of vortex flow and downwash configuration (as lift-generating, drag-reducing aspects).

4.3 Analysis of Flight Stability

The sign of the function $dM/d\alpha$ at α_0 is negative (Figure 5), indicating that out-of-trim flight attitude induces a response that restores balanced flight [4,5,13]. As a truly stable system, the ski jumper may avoid constant control movements, which create extra drag, and allow the system to settle into its trim [6,7]. Postures that are compact around the x axis, ($\lambda = 20°$ and $\theta = 0°$–$10°$) generate least restoring M and flattest $dM/d\alpha$ slope, and thus minimum response to an upset. Such postures may encourage athlete-induced oscillations (based on Nelson [3]). However, wide λ and large θ help with stability. In support of this, wide λ has been observed to reduce the speed of the downwash behind the athlete, but to broaden the effective area of downwash [13]; thus, with a weaker downwash projected over a broader area the skis are more stable. The ΔCP curves confirm that wide λ (30°) enhances static stability, which reduces T_{sp} for flight within the range $8° < \alpha < 26°$. The concomitant increase in f, although suggestive of strong static stability, may lead to dynamic oscillations if α_0 is tersely overshot [6]. Large SM also makes a direct contribution to raising f [5]. However, outside the $8° < \alpha < 26°$ range, the relatively flat $dM/d\alpha$ slopes increase T_{sp}, quenching undesirable overshoot of the α_0. T_{sp} in ski jumping is approximately 1 s longer than in small trainer aeroplanes [5]. The higher F_D generated by stable postures and the higher V_a experienced in the larger hills increase M and heavily damp the short period mode. The second statistical analysis corroborates that it is primarily F_D that fuels M, with wide λ and high F_L also arising as important stability factors. As explained by Anderson [2], any efforts to increase stability always come with an additional drag penalty. Thus, it can be suggested that a compromise is needed between a posture that yields maximum aerodynamic efficiency ($\lambda = 30°$ and $\theta = 0°$) and one that provides utmost stability ($\lambda = 30°$ and $\theta = 20°$). Fine-tuning of flight posture is attained using $\lambda = 30°$ and $\theta = 10°$, which yields the aerodynamic values shown in Table 2 as a function of V_a.

An interpretation of stability in ski jumping is suggested based on theoretical grounds [2–6] and with the aid of Figure 6, where F_D has been excluded for simplicity. The simulation data suggest that the athlete is statically stable. Thus, it is a *sine qua non* that the *NP* resides aft of the *CG*: 'An aircraft will be longitudinally stable if the CG is ahead of the NP, and vice versa' ([5]; p. 97). As an analogy, aft location of the *NP* is an essential feature of tailless aircraft due to the absence of a tailplane and longitudinal dihedral [1,4]. F_{Lcam} depends only on camber and can be considered constant. F_{Lcam} may be taken as the computed F_L at zero incidence ($\alpha = 0°$), which for the depicted posture of $\lambda = 30°$ and $\theta = 0°$ corresponds to 41 N. By completely ignoring the itinerary nature of F_L (ΔCP), we can treat F_{Linc} as acting at the *NP*, and thus have only one variable (the magnitude of F_{Linc}) that fluctuates with flight attitude (based upon Carpenter [5]). At α_0 (18°) the athlete is in rotational equilibrium, and the calculated total F_L is 233 N, of which 192 N can be attributed to incidence. However, should α abruptly decrease to 10°, F_{Linc} would drop (to 128 N), since F_{Linc} depends on α. M would increase to +11.3 Nm causing the athlete to rotate nose up about the *CG* at $\ddot{\alpha} = +0.79\ rad/s^2$. In contrast, a nose-up disturbance that increases α beyond α_0 to, for example, 30° would increase lift at the *NP* (to 254 N) causing the athlete to pitch down towards equilibrium. A flight posture defined by $\lambda = 20°$ and $\theta = 0°$ produces less F_L, M, and $\ddot{\alpha}$ (Figure 6), and is comparatively less responsive. A posture consisting of $\lambda = 30°$ and $\theta = 10°$ yields large F_{Linc} and restoring M, and is therefore more stable. Recall also that SM is longest for the latter posture (7.2 cm), thus enhancing static stability [6,7]. It can be theorized that the cambered body of the ski jumper behaves like a conventional aerofoil (unstable in pitch [1]), thus stability originates from the effect of the skis (negatively cambered profiles [11]).

β has implications for camber and therefore lift and stability [13]. However, variations in β could not be simulated, since the database of Seo *et al*. [10] is based on a straight body posture. Further insight into the contribution of individual lifting surfaces to the stability of the system can be gained through testing scaled models of single parts of the ski jumper–skis system (torso, skis) in a wind tunnel, thus expanding on the work of Reisenberger *et al*. [23]. Although lift-enhancing devices are currently not approved [17], strategically-placed boundary layer trip turbulators and invigorators may be used to control the turbulent boundary layer and vortex shedding. Such trip mechanisms may enhance stability and safety.

5. CONCLUSIONS

Trimmed flight is a highly elusive condition. However, the ski jumper triggers static stability response and tends towards equilibrium when balanced flight is upset. Increased λ enhances stability, due predominantly to aerodynamic rather

© 2009 John Wiley and Sons Asia Pte Ltd

than inertial factors. Associated with increased θ are higher I_y, which prevents diversions from trimmed attitude, and greater F_D, which provides stability augmentation. An enhanced flight posture of $\lambda = 30^\circ$ and $\theta = 10^\circ$ is suggested, independent of competition level. This is a high-lift configuration with a large SM that yields steep $dM/d\alpha$ slope and high oscillatory f, should sudden deviations from α_0 occur, and may warrant safety. High f may initiate short-lived dynamic oscillations, however. Founded upon aerodynamics theory, it is suggested that the NP is located aft of the CG in the ski jumper.

6. APPENDIX 1: EQUATIONS

6.1. Parallel axes theorem [18] and mass moment of inertia for symmetrical objects of uniform composition [19]

$$I_y = I_{CG} + md^2 \tag{1}$$

$$I_{skis} = 1/12m(l_2 + w_2) \tag{2}$$

$$I_{helmet} = 2/5mr^2 \tag{3}$$

Where I_{CG} is the local-term segmental moment of inertia, I_{skis} is the moment of inertia of the skis about the y axis, l and w stand for length and width of a rectangular thin plate, I_{helmet} is the moment of inertia of the helmet about its CG, and r is the radius of a solid sphere.

6.2 Aerodynamic drag force, lift force and pitching moment [2,10]

$$F_D = \tfrac{1}{2}\rho C_D A V_a^2 \tag{4}$$

$$F_L = \tfrac{1}{2}\rho C_L A V_a^2 \tag{5}$$

$$M = \tfrac{1}{2}\rho Q_M V_a^2 \tag{6}$$

Where

$$C_D A(\alpha,\theta,\lambda) = \sum_{i=0}^{4}\sum_{j=0}^{2}\sum_{k=0}^{2} a_{ijk}\ \alpha^i\theta^j\lambda^k$$

$$C_L A(\alpha,\theta,\lambda) = \sum_{i=0}^{4}\sum_{j=0}^{2}\sum_{k=0}^{2} b_{ijk}\ \alpha^i\theta^j\lambda^k$$

$$Q_M(\alpha,\theta,\lambda) = \sum_{i=0}^{4}\sum_{j=0}^{2}\sum_{k=0}^{2} c_{ijk}\ \alpha^i\theta^j\lambda^k$$

and a_{ijk}, b_{ijk}, and c_{ijk} are coefficients.

6.3 Reynolds number

$$Re = (V_a \bullet \ell)/(\mu/\rho) \tag{7}$$

Where ℓ is the reference length of 0.126 m based on the approximate thickness of the upper body, as in previous investigation [23], and μ is the coefficient of viscosity [12] at a particular T (in Kelvin) as follows:

$$\mu = 1.458 \times 10^{-6}(T^{1.5}/[T + 110.4])$$

6.4 Equations of motion of the ski jumper [15]

$$\delta V_x = (-F_D \cos\varphi - F_L \sin\varphi)/m \tag{8}$$

$$\delta V_y = ([-F_D \sin\varphi - F_L \cos\varphi]/m) - g \tag{9}$$

Where V_x and V_y are the horizontal and vertical components of projectile velocity, respectively, m represents the mass of the ski jumper and equipment, and g is the gravitational constant of 9.80665 m/s^2.

6.5 Centre of pressure shift (based on Anderson [2])

$$\Delta CP = M([[F_L^2 + F_D^2]^{0.5}] \times \sin[[\tan^{-1}[F_L/F_D]] + \alpha + \theta]) \tag{10}$$

6.6 Angular acceleration for out-of-trim flight [3]

$$\ddot{\alpha} = M/I_y \tag{11}$$

6.7 Static margin (based on Carpenter [5])

$$SM = dM/d\alpha \times \text{ski length} \tag{12}$$

Where SM is in centimeters, and ski length is used as the mean chord length of the ski jumper-skis system and is entered in meters.

6.8 Period of the short-period mode of the pitching oscillation [3,10]

$$T_{sp} = 2\pi(-1/M_\alpha)^{0.5} \tag{13}$$

Where π is the ratio 3.14159 and $M_\alpha = (dM/d\alpha)/2I_y$, whereby M_α is the pitching moment derivative normalized by I_y.

6.9 Frequency of the short-period pitching oscillation [5]

$$f = 1 \text{ cycle}/T_{sp} \tag{14}$$

REFERENCES

1. Kermode AC. *Mechanics of Flight*. Pearson Education Ltd: London. 2006.
2. Anderson JD. *Fundamentals of Aerodynamics*. McGraw-Hill: London. 2007.
3. Nelson RC. *Flight Stability and Automatic Control*. McGraw Hill: New York. 1998.
4. Simons M. *Model Aircraft Aerodynamics*. Special Interest Model Books Ltd: Dorset. 2002.
5. Carpenter C. *Flightwise: Aircraft Stability and Control*. Airlife: Shrewsbury. 1997.

 © 2009 John Wiley and Sons Asia Pte Ltd

6. Milne-Thomson LM. *Theoretical Aerodynamics*. Dover Publications Inc: New York. 1973.

7. Thomas AL, Taylor GK. Animal flight dynamics I: Stability in gliding flight. *Journal of Theoretical Biology* 2001; **212**: 399–424.

8. Meile W, Reisenberger E, Mayer M, Schmölzer B, Müller W, Brenn G. Aerodynamics of ski jumping: Experiments and CFD simulations. *Experiments in Fluids* 2006; **41**: 949–964.

9. Schwameder H. Biomechanics research in ski jumping, 1991–2006. *Sports Biomechanics* 2008; **7**(1): 114–136.

10. Seo K, Watanabe I, Murakami M. Aerodynamic force data for a V-style ski jumping flight. *Sports Engineering* 2004; **7**: 31–39.

11. Katz J. *New Directions in Race Car Aerodynamics*: *Designing for Speed*. Bentley Publishers: Cambridge, Massachusetts. 2006.

12. Bertin JJ. *Aerodynamics for Engineers*. Prentice Hall: New Jersey. 2002.

13. Ito S, Seo K, Asai T. An experimental study on ski jumping styles. In: Estivalet M, Brisson B (Eds.). *The Engineering of Sport 7*, Vol. 2, Springer: Paris, 2008; 9–18.

14. Müller W, Platzer D, Schmölzer B. Scientific approach to ski safety. *Nature* 1995; **375**: 455.

15. Müller W, Platzer D, Schmölzer B. Dynamics of human flight on skis: Improvements in safety and fairness in ski jumping. *Journal of Biomechanics* 1996; **29**(8): 1061–1068.

16. Müller W. Biomechanics of ski-jumping: Scientific jumping hill design. In: Müller E, Schwameder H, Kornexl E, Raschner C (Eds.). *Science and Skiing*, E & EF Spon: London, 2003; 36–48.

17. Fédération Internationale de Ski. *The International Ski Competition Rules. Book III– Ski jumping*. Oberhofen: Switzerland. 2004.

18. Zatsiorsky VM. *Kinetics of Human Motion*. Human Kinetics: Champaign, Illinois. 2002.

19. Griffiths IW. *Principles of Biomechanics and Motion Analysis*. Lippincott: Williams & Wilkins, London. 2006.

20. Dumas R, Cheze L, Verriest JP. Adjustments to McConville *et al.* and Young *et al.* body segment inertial parameters. *Journal of Biomechanics* 2007; **40**: 543–553.

21. Murakami M, Hirai N, Seo K, Ohgi Y. Aerodynamic forces computation from high-speed video image of ski jumping flight. In: Fuss FK, Subic A, Ujihashi S (Eds.). *The Impact of Technology on Sport II*, Taylor and Francis Group: London, 2008; 857–862.

22. Yeadon MR. The simulation of aerial movement II: A mathematical inertia model of the human body. *Journal of Biomechanics* 1990; **23**(1): 67–74.

23. Reisenberger E, Meile W, Brenn G, Müller W. Aerodynamic behaviour of prismatic bodies with sharp and rounded edges. *Experiments in Fluids* 2004; **37**: 547–558.

24. Smith RT, Minton RB. *Calculus*. McGraw-Hill: New York. 2002.

25. Shiavi R. *Introduction to Applied Statistical Signal Analysis*: *Guide to Biomedical and Electrical Engineering Applications*. Academic Press: London. 2007.

26. Tabachnick BG, Fidell LS. *Using Multivariate Statistics*. Allyn and Bacon: London. 2001.

Received 2 December 2008
Revised 16 January 2009
Accepted 19 January 2009

 © 2009 John Wiley and Sons Asia Pte Ltd